A Vascular Endothelial Growth Factor Receptor-2 Inhibitor Enhances Antitumor Immunity through an Immune-Based Mechanism

Elizabeth A. Manning,[1,2] John G.M. Ullman,[1,3] James M. Leatherman,[1,3] Justin M. Asquith,[1,3] Timothy R. Hansen,[1,3] Todd D. Armstrong,[1,3] Daniel J. Hicklin,[7] Elizabeth M. Jaffee,[1,2,3,4,5,6] and Leisha A. Emens[1,3]

Abstract

Purpose: Given the complex tumor microenvironment, targeting multiple cellular components may be the most effective cancer treatment strategy. Therefore, we tested whether antiangiogenic and immune-based therapy might synergize by characterizing the activity of DC101, an antiangiogenic monoclonal antibody specific for vascular endothelial growth factor receptor-2 (VEGF-R2), alone and with HER-2/*neu* (neu) – targeted vaccination.

Experimental Design: Neu-expressing breast tumors were measured in treated nontolerant FVB mice and immune-tolerant *neu* transgenic (*neu*-N) mice. Neu-specific and tumor cell – specific immune responses were assessed by intracellular cytokine staining, ELISPOT, and CTL assays.

Results: DC101 decreased angiogenesis and increased tumor cell apoptosis. Although DC101 increased serum levels of the immunosuppressive cytokine VEGF, no evidence of systemic immune inhibition was detected. Moreover, DC101 did not impede the influx of tumor-infiltrating lymphocytes. In FVB mice, DC101 inhibited tumor growth in part through a T cell – dependent mechanism, resulting in both increased tumor-specific $CD8^+$ T cells and tumor regression. Combining DC101 with neu-specific vaccination accelerated tumor regression, augmenting the lytic activity of $CD8^+$ cytotoxic T cells. In tolerant *neu*-N mice, DC101 only delayed tumor growth without inducing frank tumor regression or antigen-specific T-cell activation. Notably, mitigating immune tolerance by inhibiting regulatory T cell activity with cyclophosphamide revealed DC101-mediated augmentation of antitumor responses in vaccinated *neu*-N mice.

Conclusions: This is the first report of DC101-induced antitumor immune responses. It establishes the induction of tumor-specific T-cell responses as one consequence of VEGF-R2 targeting with DC101. These data support the development of multitargeted cancer therapy combining immune-based and antiangiogenic agents for clinical translation.

Authors' Affiliations: [1]The Sidney Kimmel Comprehensive Cancer Center at Johns Hopkins, The Johns Hopkins University School of Medicine, Baltimore, Maryland; Departments of [2]Pharmacology and Molecular Sciences and [3]Oncology, Graduate Programs in [4]Immunology and [5]Cellular and Molecular Medicine, and [6]Department of Pathology, and [7]Experimental Therapeutics, ImClone Systems Inc., New York, New York

Received 2/13/07; revised 3/31/07; accepted 4/13/07.

Grant support: The Department of Defense (W81XWH-04-1-0595) to E.M. Jaffee and L.A. Emens; the National Cooperative Drug Discovery Groups (U19CA72108), the Breast Specialized Programs of Research Excellence (P50CA88842), the Komen Foundation, and the Alliance for Cancer Gene Therapy (to E.M. Jaffee); NIH (K23 CA098498), the Department of Defense (DAMD17-01-1-0281), and Maryland Cigarette Restitution Fund (M020216; to L.A. Emens); and NIH (training grant CA09243; to E.A. Manning).

The costs of publication of this article were defrayed in part by the payment of page charges. This article must therefore be hereby marked *advertisement* in accordance with 18 U.S.C. Section 1734 solely to indicate this fact.

Conflict of interest statement: This work describes the use of a granulocyte macrophage colony-stimulating factor – secreting tumor vaccine. Although none of the authors have financial interests in the work, the Johns Hopkins University receives milestone payments and has the potential to receive royalties in the future.

Requests for reprints: Leisha A. Emens, Room 4M90, Bunting-Blaustein Cancer Research Building, 1650 Orleans Street, Johns Hopkins University, Baltimore, MD 21231. Phone: 410-502-7051; Fax: 410-614-8216; E-mail: emensle@jhmi.edu.

doi:10.1158/1078-0432.CCR-07-0374

Signaling pathways involved in transformation and tumor progression are key targets for cancer therapy. Because tumors are heterogeneous, with high mutation rates that activate compensatory pathways or facilitate acquired resistance to single therapies, multitargeted strategies may represent optimal cancer treatments.

Tumor immunotherapy can specifically target tumor-associated antigens, resulting in low toxicity and the potential for durable immunologic memory responses. Because tumor cells arise endogenously, most tumor antigens may be recognized as self. Consequently, tumor-specific T cell repertoires may be limited through mechanisms of central (thymic deletion) or peripheral tolerance [deletion, ignorance, anergy, or suppression by $CD4^+CD25^+$ regulatory T cells (Treg); ref. 1]. Because immunotherapy alone may not be successful against advanced disease, it is important to investigate combinatorial strategies for augmenting the potency of cancer vaccines.

Several studies support integrating tumor immunotherapy and antiangiogenic therapy (2–4). Angiogenesis, defined as the development of new vasculature from preexisting blood vessels, is involved in tumor growth and metastasis (5). The success of Bevacizumab (Avastin), the first Food and Drug

Administration – approved antiangiogenic therapy, shows the importance of targeting angiogenesis (6). However, antiangiogenic therapy often requires continuous drug administration, and residual tumor masses may be capable of regrowth (7). These findings reiterate the need for multitargeted therapy. Therefore, we sought to examine clinically relevant interactions between tumor immunotherapy and antiangiogenic therapy in the HER-2/*neu* (neu) mouse model.

The proto-oncogene neu is overexpressed in up to 25% of human breast cancers and confers a poor prognosis (8). *Neu*-N mice, derived from the parental FVB strain, express nontransforming rat *neu* cDNA under the control of the mammary-specific promoter mouse mammary tumor virus (9). Consequently, *neu*-N mice spontaneously develop mammary cancers and exhibit well-established peripheral immune tolerance to neu (10). Neu-specific whole-cell granulocyte macrophage colony-stimulating factor (GM-CSF) – secreting vaccines induce curative neu-specific immune responses in tumor-bearing FVB mice, with most neu-specific $CD8^+$ T cells recognizing the MHC class I epitope $RNEU_{420-429}$ (11). Conversely, neu-specific vaccines alone are ineffective in tolerant *neu*-N mice. We have shown that modulating immune checkpoints can improve antitumor responses. Administering low-dose cyclophosphamide before vaccination abrogates the immunosuppressive effects of Tregs, leading to the expansion of high-avidity, $RNEU_{420-429}$ – specific $CD8^+$ T cells and prolonged tumor-free survival in up to 30% of *neu*-N mice (12). Similar results were observed with OX40 (CD134) costimulation (13).

Neu overexpression correlates with increased angiogenesis and expression of vascular endothelial growth factor (VEGF). VEGF, which is produced by tumors and endothelial cells, can promote both angiogenesis (14) and immune suppression (15). VEGF signals in part via VEGF receptor-2 (VEGF-R2; Flk1/KDR), a transmembrane tyrosine kinase receptor whose expression is predominantly localized to vascular endothelial cells (14), and correlates with invasion and metastasis (16). Therefore, various VEGF-R2 inhibitors are being developed (17). One example is DC101, a rat monoclonal antibody specific for mouse VEGF-R2 that can significantly decrease tumor growth and angiogenesis *in vivo* (18, 19).

Given the importance of neu and VEGF in tumor progression, and their potential biological interactions, we investigated the bioactivity of DC101-mediated VEGF-R2 inhibition alone and combined with neu-specific vaccination. We first examined the effects of DC101 on tumor angiogenesis and apoptosis and then determined whether DC101 treatment might result in VEGF-mediated immune suppression or impaired T cell infiltration into tumors. We then characterized antitumor immunity and tumor regression after DC101 administration, comparing DC101-induced responses in nontolerized FVB mice and tolerized *neu*-N mice. Here, we show for the first time that DC101 can enhance antitumor responses by improving tumor-specific T-cell activity in the absence of immune tolerance.

Materials and Methods

Mice. FVB mice were purchased from Harlan or Taconic Laboratories. *Neu*-N mice (9), provided by Dr. William Muller (McGill University, Montreal, Canada), were bred to homozygosity as verified by Southern blot (10). The colony was maintained at Harlan Biotech Center (Baltimore, MD).

Clone 100 T-cell receptor (TCR) transgenic mice, derived from FVB mice, express the high-avidity, $RNEU_{420-429}$ – specific TCR in the majority of peripheral $CD8^+$ T cells. Briefly, mice were generated by cloning cDNA from high-avidity, $RNEU_{420-429}$ – specific T cell lines (12) into TCR α and β chain constructs, followed by ligation into corresponding TCR cassette vectors using previously described methods (20, 21). The linearized DNA fragments were microinjected into fertilized eggs, which were then implanted into pseudopregnant FVB mice in the Johns Hopkins Medical Institutions transgenic core. Flow-cytometric analysis of founder mice confirmed that >95% of peripheral $CD8^+$ T cells contained Vβ4 sequences and 60% to 70% were also specific for $RNEU_{420-429}$.[8]

The generation of p56*lck*GFP mice has been described (22). The pEGFP-C1 gene (Clonetech), ligated to the *lck* proximal promoter, was microinjected into fertilized FVB eggs. Flow-cytometric data confirmed >95% GFP^+ T cells (data not shown).

Experiments were done with 8- to 12-week-old mice using AAALAC-compliant protocols approved by the Animal Care and Use Committee of the Johns Hopkins University School of Medicine.

Cell lines and media. The GM-CSF – secreting vaccine cell lines 3T3GM (mock) and 3T3neuGM (neu-specific), the NT2.5 neu-expressing breast tumor cell line (derived from a spontaneous tumor explanted from a *neu*-N mouse), and the $T2D^q$ line were grown as previously described (10). The 3T3neuB7.1 and NT2.5B7.1 lines were produced via retroviral transduction with a human B7.1-encoding retrovirus (23). The pancreatic endothelial cell line MS-1 [American Type Culture Collection (ATCC)] was grown in ATCC medium [DMEM with 4 mmol/L L-glutamine, 1.5 g/L sodium bicarbonate, 4.5 g/L glucose, and 5% fetal bovine serum (FBS)].

RNA isolation, cDNA preparation and reverse transcription-PCR. RNA was isolated (RNeasy Mini; Qiagen Inc.), followed by cDNA preparation [Superscript First-Strand Synthesis System for Reverse Transcription-PCR (RT-PCR), Invitrogen Corp.]. cDNA amplification used the following primers: VEGF sense, GAGATCCTTCGAGGAGCACTT, and antisense, GCGATTTAGCAGCAGATATAAGA; VEGF-R2 sense, TACACAATTCAGAGCGATGTGTGGT, and antisense, CTGGTTCC-TCCAATGGGATATCTTC (Invitrogen). Reaction conditions included a 2-min denaturation at 94°C, followed by 30 cycles of 94°C – 30 s/65°C – 30 s/72°C – 60 s, and a final 7-min extension at 72°C. Glyceraldehyde-3-phosphate dehydrogenase (GAPDH) served as a control, using primers and protocols from Applied Biosystems. PCR products were analyzed by electrophoresis in a 1.5% agarose gel.

Antibody administration. DC101 was supplied by Dr. Daniel Hicklin (ImClone Systems Inc., New York, NY). Nonspecific polyclonal rat immunoglobulin G (IgG; Sigma-Aldrich, St. Louis, MO) served as a control. Antibodies were endotoxin free, as confirmed in-house by the *Limulus* amebocyte lysate test (Bio Whittaker, Walkersville, MD). Antibodies were diluted in 250 μL PBS and injected i.p. at 0.8 mg per mouse twice weekly as previously described (18, 19).

Immunohistochemistry. OCT-coated tumors (Tissue-Tek, VWR) were snap frozen and sectioned at 5 μm at the JHMI Pathology Core. Sections were stained with H&E or retained for immunohistochemistry using reagents and protocols from BD Bioscience. Vascularization and apoptosis were analyzed with antibodies specific for PECAM/CD31 and cleaved caspase-3, respectively (BD PharMingen), and slides were developed with 3,3′-diaminobenzidine (DAKO Incorporated). Images were captured under light microscopy (E800, Nikon) at 20× magnification. Quantification of PECAM staining was done by digital densitometry using MetaMorph software via TopHat analysis (Molecular Devices Corp.).

VEGF ELISA. NT2.5 cells were seeded at 10^6 cells/mL in a six-well plate, and supernatant was harvested 24 h later. Blood was harvested from mice by cardiac puncture, and serum was collected by centrifugation. Supernatant and serum were analyzed by VEGF ELISA (R&D Systems).

[8] T.D. Armstrong, unpublished data.

Antibodies, flow cytometry (fluorescence-activated cell sorting) analysis, and tetramer staining. Anti–CD3-FITC, anti–CD62L-FITC, anti–B7.1-FITC, anti–B7.2-FITC, anti–Gr1-FITC, anti–CD8-CyChr, anti–CD4-PE, anti–CD11c-PE and anti–Mac1-PE were used to stain leukocytes (BD PharMingen). NT2.5 cells were stained with serially diluted serum harvested from tumor-bearing mice, followed by a PE-labeled anti-mouse IgG antibody (BD PharMingen). The H-2D^q-RNEU$_{420\text{-}429}$ tetramer was constructed and used to stain splenic T cells as previously described (12, 24). Fluorescence-activated cell sorting data was collected using a BD FACScan with CellQuest software (BD Bioscience) and analyzed with FlowJo software (TreeStar, Inc.).

Tumor treatment experiments and chemotherapy. FVB mice were challenged s.c. with 5×10^6 NT2.5 tumor cells in the right mammary fat pad, followed by vaccination 14–28 days later. *Neu*-N mice were challenged with 5×10^4 NT2.5 cells and vaccinated 3 days later. Vaccine cells were irradiated before s.c. injection in both hind limbs and the left front limb. Cyclophosphamide (Bristol-Myers Squibb) was injected i.p. at 100 mg/kg 1 day before the vaccine. Doxorubicin (Gensia Sicor) was injected i.v. at 5 mg/kg 7 days after vaccine. Doses and timing for tumor cells, vaccinations, and chemotherapy have been previously optimized and reported (10, 25). Mice were monitored for tumor growth and onset twice weekly. Tumor growth was determined by measuring tumor diameter in two perpendicular dimensions with calipers. Tumor size was calculated by multiplying these two measurements. Mean tumor size for an experimental group included only those mice with measurable tumors.

Ex vivo *antigen presentation assay.* Tumor-bearing FVB mice received a 2-week course of DC101 or rIgG, followed by vaccination. One week postvaccination, splenic dendritic cells (DC) were harvested, purified over a Nycodenz gradient (Accurate Chemical), depleted of CD3$^+$ and CD19$^+$ cells (Dynal Biotech, Invitrogen), and enriched for CD11c$^+$ cells (Miltenyi Biotech). Clonotypic CD8$^+$ cells were isolated from Clone 100 TCR transgenic mice by negative selection (Dynal Biotech), and labeled with carboxyfluoroscein succinimidyl ester (CFSE; Molecular Probes, Invitrogen). Purified DCs (10^5 per well) were cocultured with naïve CFSE-labeled CD8$^+$ cells (10^5 per well) in a 24-well plate for 4 days, and CFSE dilution was measured by flow cytometry.

Intracellular cytokine staining. RNEU$_{420\text{-}429}$ (PDSLRDLSVF) and NP$_{118-126}$ (RPQASGVYM) peptides were synthesized at >95% purity by the Oncology Peptide Synthesis Facility (Johns Hopkins, Baltimore, MD). Intracellular cytokine staining (ICS) was conducted as previously described (12). The percent of antigen-specific CD8$^+$ T cells is given as the percent of IFN-γ$^+$ cells in the irrelevant NP$_{118\text{-}126}$ sample subtracted from that in the neu-specific RNEU$_{420\text{-}429}$ sample.

ELISPOTS. CD8$^+$ splenic lymphocytes were purified by negative selection (Dynal Biotech). About 10^5 CD8$^+$ T cells were incubated in duplicate with 10^4 target cells (NT2.5B7.1 cells stimulated with IFN-γ for 2 days) at 37°C overnight on precoated IFN-γ–specific ELISPOT plates and developed according to manufacturer's protocols (R&D Systems). IFN-γ–secreting CD8$^+$ T cells were enumerated using the Immunospot counter (Cellular Technology, Ltd.). The average number of spots in control wells was subtracted from the average number of spots in each well containing both CD8$^+$ T cells and targets.

In vivo *depletions.* CD4$^+$ and CD8$^+$ T cells were continuously depleted using GK1.5 and 2.43 antibodies, respectively, as previously described (10), except that filtered, diluted ascites was used. Natural killer cells and macrophages were depleted by twice weekly i.p. injections of α-asialo GM1 (Wako Chemical) and carrageenan (Sigma-Aldrich), respectively. Greater than 95% depletion was confirmed by flow cytometry.

Chromium-release assays. Splenic lymphocytes were isolated by Ficoll gradient centrifugation (Amersham Bioscience), and their lytic activity against NT2.5B7.1 and 3T3neuB7.1 target cells was tested in triplicate in a standard 4-h chromium-release assay as previously described (12). The percent specific lysis was determined using the following formula: (experimental release - spontaneous release)/(maximum release - spontaneous release) × 100.

Isolation and characterization of tumor-infiltrating lymphocytes. Tumors from p56*lck*GFP FVB mice were prepared as described above. Unstained sections were visualized by fluorescence microscopy (E800, Nikon) at 20× magnification. GFP$^+$ cells were quantified using MetaMorph software via TopHat analysis.

Tumors from FVB mice were weighed and digested into single-cell suspensions with hyaluronidase, collagenase type IV and trypsin (Life Technologies, Invitrogen) using standard methods. Cells were plated for 2 to 3 h to allow tumor cells to adhere, and then the T cell–enriched supernatant was collected. Cells were counted, analyzed by flow cytometry, and normalized to tumor weight.

Statistical analysis. A Student's *t*-test was applied to determine the statistical significance of differences between treatment groups, with $P < 0.05$ being significant. Analyses were done using GraphPad Prism, version 3.0a for Macintosh (GraphPad Software). All experiments were repeated at least twice, with 5 to 20 mice per group depending on the study end point.

Results

DC101 inhibits tumor growth, decreases angiogenesis, and increases tumor cell apoptosis in neu-expressing tumors. We first examined the expression of VEGF and VEGF-R2 in FVB and *neu*-N mice. The neu-overexpressing NT2.5 breast tumor cell line secreted VEGF at ~150 pg/10^6 cells/24 h (data not shown). VEGF-R2 mRNA was not detected in these cells, but was measurable in normal mammary tissue and seemed to be increased in transplanted and spontaneous tumors (Fig. 1A). These explanted tumor samples contain both tumor and surrounding endothelial cells, suggesting that VEGF-R2 is up-regulated within the microenvironment of neu-expressing tumors *in vivo*.

The administration of DC101 to tumor-bearing FVB mice significantly inhibited the growth of neu-expressing tumors (Fig. 1B). Tumors from DC101-treated mice were necrotic (Fig. 1C). Immunohistochemistry showed that DC101 reduced angiogenesis and increased tumor cell death (Fig. 1C). Specifically, the amount of endothelial cell–specific PECAM staining was decreased by 81% ($P = 0.006$) in tumors treated for 2 weeks with DC101 as compared with rIgG. These data confirm the known antiangiogenic activity of DC101.

DC101 treatment does not induce VEGF-mediated immune suppression or impede the influx of tumor-infiltrating lymphocytes. Although VEGF levels often correlate with tumor burden, DC101 treatment increases systemic VEGF levels, even when tumor growth is inhibited (26). This increase may be due to reduced receptor-mediated endocytosis of VEGF as DC101 blocks VEGF-R2 or increased tumor-derived VEGF to compensate for diminished signaling. Although the VEGF ELISA assay has some cross-reactivity with circulating DC101, we found serum VEGF levels increased by almost 5-fold in DC101-treated tumor-bearing FVB mice, consistent with a bona fide elevation in VEGF (Fig. 2A).

Although elevated VEGF levels correlate with increased levels of T cell–suppressive immature myeloid cells (MSC), (27), MSC were not significantly expanded in DC101-treated FVB mice (Fig. 2B). Similarly, although VEGF can inhibit the maturation of DCs (28–30), DC101-induced VEGF did not inhibit DC maturation as measured by the expression of the costimulatory markers B7.1 and B7.2 (data not shown). Furthermore, activated DCs harvested from vaccinated FVB mice pretreated with DC101 or rIgG were equally able to stimulate the proliferation of naïve RNEU$_{420\text{-}429}$–specific clonotypic CD8$^+$ T

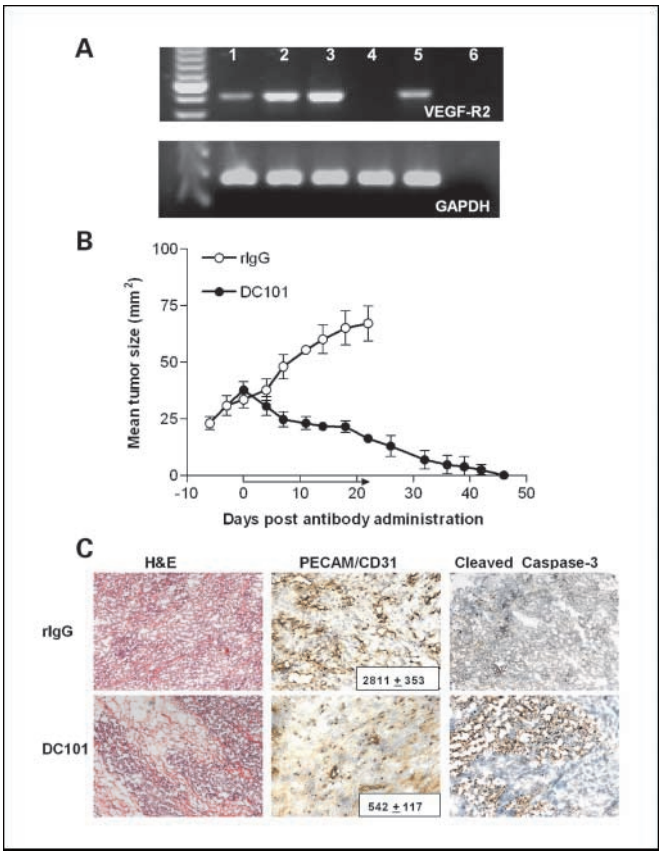

Fig. 1. DC101 inhibits tumor growth, decreases angiogenesis, and increases apoptosis within tumors of FVB mice. *A,* RT-PCR was conducted with gene-specific primers for VEGF-R2 and GAPDH. Lane 1, normal mammary tissue; lane 2, transplanted tumor; lane 3, spontaneous tumor; lane 4, NT2.5 tumor cells; lane 5, MS-1 endothelial cells; lane 6, no cDNA. *B,* FVB mice ($n = 20$ per group) were tumor challenged and 2 wks later began receiving rIgG or DC101 biweekly for 3 wks (*horizontal arrow*). *C,* tumors from FVB mice were prepared for histologic examination 2 wks after antibody administration as described in (*B*). Representative samples of mice treated with rIgG (*top*) or DC101 (*bottom*) are shown with H&E staining or immunohistochemistry to detect endothelial cells (PECAM/CD31) or apoptotic cells (cleaved caspase-3), at 20× magnification. PECAM staining was quantified using MetaMorph software. Numbers (mean + SD) are the densitometry values from three samples per group.

cells from TCR transgenic mice (Fig. 2C). The frequency and avidity of $CD8^+$ T cells specific for $RNEU_{420-429}$ were also comparable between the two groups (Fig. 2D and E). Therefore, whereas DC101 administration increased VEGF levels *in vivo*, DC-dependent immune priming was not impaired, and no evidence of functional $CD8^+$ T cell suppression was detected.

We next analyzed tumor-infiltrating lymphocytes (TIL) to determine if T cells could still effectively traffic to DC101-treated tumors. Two weeks after the DC101 treatment of tumor-bearing p56*lck*GFP FVB mice (alone or before vaccination), increased numbers of TIL were detected by fluorescence microscopy (Fig. 3A and B). GFP^+ T cells were not found in the kidney (an irrelevant control), demonstrating that T cells traffic to the tumor after DC101 treatment. Flow-cytometric analysis revealed greater numbers of $CD4^+$ and $CD8^+$ T cells within the tumors of FVB mice treated with DC101 (Fig. 3C). These observations show that DC101 administration does not restrict, and may facilitate, T cell trafficking to the tumor. Therefore, DC101 treatment does not negatively impact functional host immune responses or T cell trafficking.

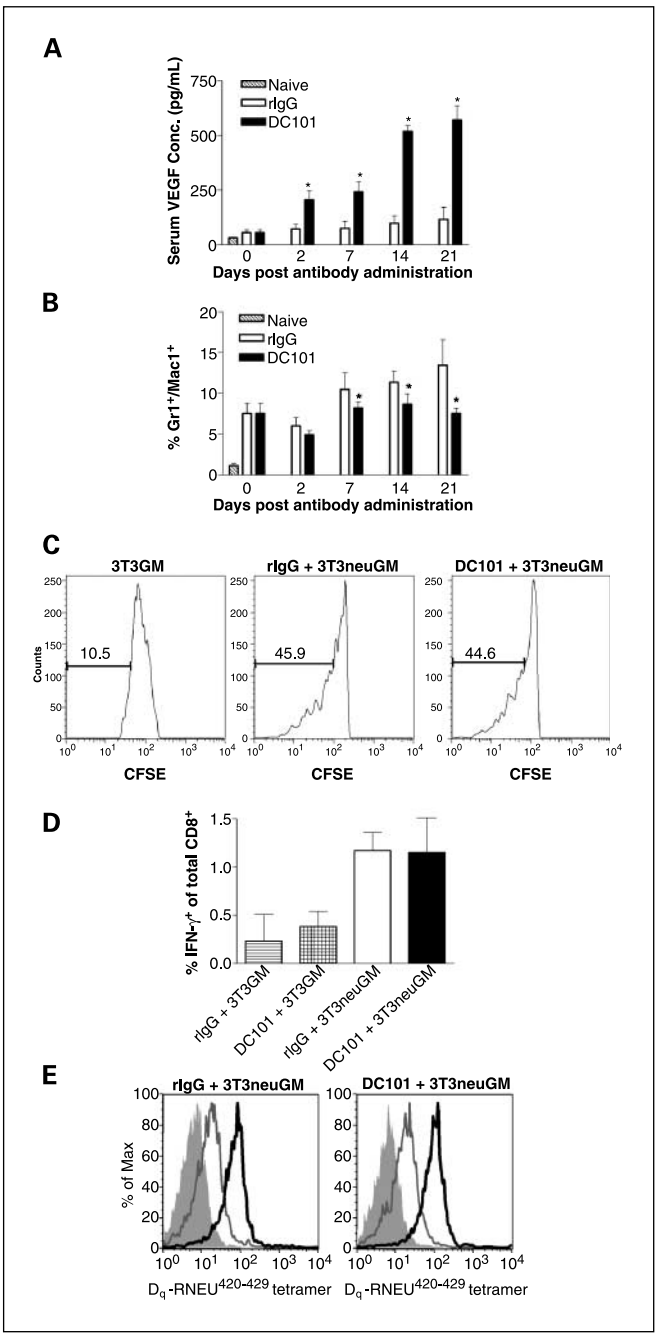

Fig. 2. DC101 administration increases serum VEGF levels, but does not cause immune suppression or inhibit vaccine-induced immunity in FVB mice. *A,* FVB mice were tumor challenged and then given rIgG or DC101 biweekly beginning 2 wks later. At various time points ($n = 5$ per group), serum VEGF levels were quantified by ELISA. *, $P < 0.05$. *B,* splenocytes were harvested from mice in (*A*) and analyzed by flow cytometry using antibodies specific for immature myeloid cell markers Gr1 and Mac1. *, $P < 0.05$. *C,* tumor-bearing FVB mice ($n = 5$ per group) received a 2-wk course of DC101 or rIgG, followed by neu-specific vaccination (3T3neuGM) or mock vaccination (3T3GM). Splenic DCs harvested 1 wk after vaccination were cocultured with naïve CFSE-labeled $RNEU_{420-429}$–specific $CD8^+$ T cells from Clone 100 TCR transgenic mice for 4 d. T-cell proliferation was analyzed by CFSE dilution. Representative samples from each group are shown. *D,* additional FVB mice ($n = 5$ per group) were treated as described in (*C*). Splenic T cells were isolated 2 wks after vaccination, and reactivity to the immunodominant $RNEU_{420-429}$ epitope was determined by IFN-γ ICS. *E,* splenic T cells were also stained with CD8, CD62L, and D^q-$RNEU_{420-429}$ tetramer. Histograms show representative samples from each group, with gating on the $CD8^+$, $CD62L^{lo}$ cells stained with decreasing dilutions of D^q-$RNEU_{420-429}$ tetramer. Black solid line, 1:5 tetramer dilution; gray line, 1:50 tetramer dilution; shaded, 1:500 tetramer dilution.

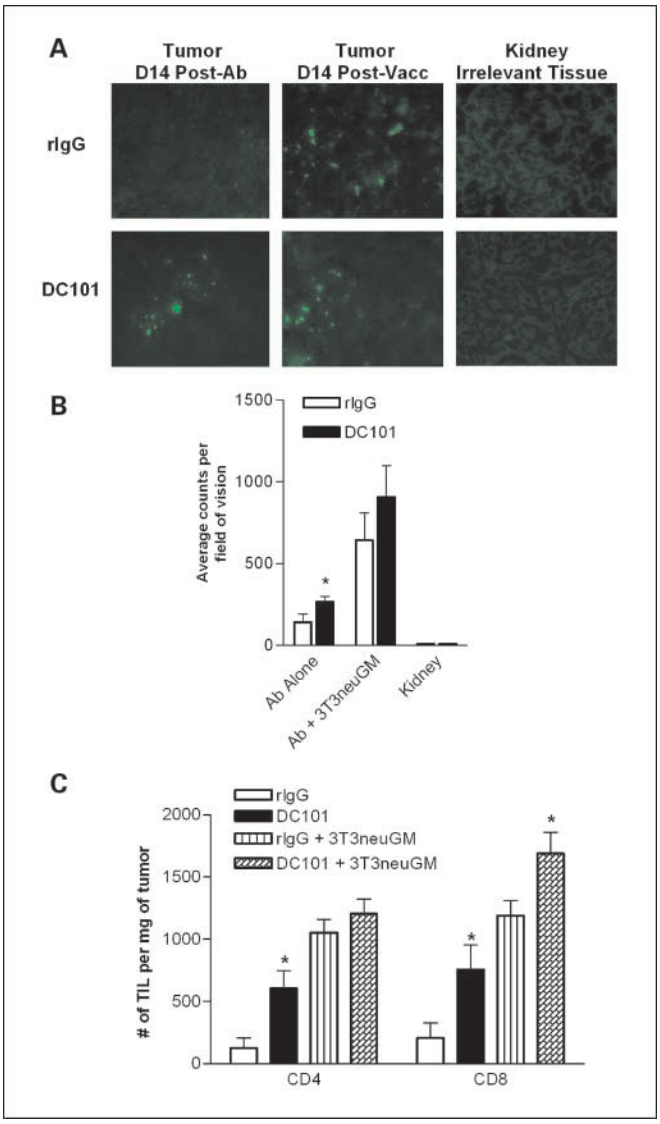

Fig. 3. DC101 administration improves T cell infiltration into the tumors of FVB mice. *A,* tumors from p56*lck* GFP FVB mice ($n = 5$ per group) were harvested either 2 wks after antibody administration or 2 wks after vaccination with antibody pretreatment. Irrelevant tissue from kidney was used as a negative control. GFP was visualized by fluorescence microscopy at 20× magnification. *B,* the images were quantified using MetaMorph software. At least two fields of vision per slide were analyzed. *, $P < 0.05$. *C,* additional tumor samples from FVB mice ($n = 5$ per group) were harvested 3 wks after antibody alone or 2 wks after vaccination with antibody pretreatment. The tumors were digested and the T cell – enriched fraction was isolated and stained with antibodies specific for CD4 and CD8. Samples were analyzed by flow cytometry, with the number of positive cells normalized to tumor weight. *, $P < 0.05$.

DC101 inhibits tumor growth through a T cell–dependent mechanism and enhances antitumor immune responses in FVB mice. Potential immune-based antitumor effects of DC101 were first examined in nontolerant FVB mice, where the neu tumor antigen is highly immunogenic. Systemic DC101 given for 3 weeks significantly reduced the size of established tumors (day 0: 28.1 ± 5.5 mm^2; day 21: 18.8 ± 5.8 mm^2; $P < 0.05$; Fig. 4A). Notably, DC101 stabilized tumor growth without inducing regression in T cell–depleted mice (day 0: 33.9 ± 6.06 mm^2; day 21: 31.07 ± 7.04 mm^2; $P = 0.20$). Selective depletion of CD4+ and/or CD8+ T cells revealed that the DC101-mediated antitumor effect was dependent on both subsets (Fig. 4A). Natural killer cell or macrophage depletion did not impact the antitumor effect of DC101 (data not shown). After discontinuing DC101 treatment, tumors resumed growth only in T cell–depleted mice (Fig. 4A). Collectively, these data show that DC101 can facilitate T cell–dependent tumor regression in addition to mediating an antiangiogenic effect (Fig. 1C).

DC101-mediated T cell responses were also investigated. We found a significant expansion of tumor-specific $CD8^+$ and $CD4^+$ T lymphocytes in FVB mice treated for 1 to 3 weeks with DC101 compared with rIgG (Fig. 4B and C). Withdrawing DC101 after a 3-week treatment period revealed that only immune-competent FVB mice completely rejected their tumors (data not shown). Upon rechallenge, one-half of these cured mice remained tumor free, with most of them developing $RNEU_{420-429}$–specific $CD8^+$ T cell responses almost as well as neu-vaccinated FVB controls (Fig. 4D). Antitumor antibody titers in mice treated with rIgG or DC101 were similar (data not shown). Although B cells may contribute, these data suggest that DC101 induces T cell–mediated tumor rejection and tumor-specific immune responses in nontolerant tumor-bearing hosts.

Combining DC101 with neu-specific vaccination in FVB mice is effective. Because DC101 alone augmented antitumor responses in FVB mice, we examined DC101 in combination with neu-targeted vaccination. Tumors regressed faster in neu-vaccinated mice pretreated for 2 weeks with DC101 compared with rIgG-treated neu-vaccinated controls (Fig. 5A, $P = 0.004$). To equalize the extent of tumor burden at the time of vaccination, antibody treatment was alternatively begun the day of vaccination. Here, there was a significant difference in the rate of tumor regression between mock-vaccinated mice and neu-vaccinated mice in the setting of DC101 treatment (Fig. 5B, $P < 0.001$). However, the difference between the rIgG- and DC101-treated mice in the setting of neu-targeted vaccination was not statistically significant (Fig. 5B, $P = 0.086$). This may be due to the ability of the neu-specific vaccine to induce robust antitumor immune responses in FVB mice. Nevertheless, neu-vaccinated mice did seem to reject tumors sooner in the setting of DC101 treatment because the time to reach 50% tumor free was shorter (18 versus 25 days posttreatment, respectively).

Significant increases in CTL activity against NT2.5 tumor cells and 3T3neu target cells were detected in neu-vaccinated mice that also received DC101 (Fig. 5C and D). Interestingly, whereas immune responses specific for $RNEU_{420-429}$ remained unchanged after combination therapy (Fig. 2D and E), enhanced T cell activity was seen against whole tumor cells and full-length neu (Fig. 5C and D). This suggests that combining DC101 and vaccination may induce a more heterogeneous repertoire of T cells, recognizing tumor-specific epitopes other than $RNEU_{420-429}$. Together, these data show that DC101 can be effectively incorporated into a tumor vaccine regimen, leading to improved tumor-specific immune responses.

DC101-induced antitumor responses are only detected in* neu-*N mice after inhibition of Tregs with immune modulating doses of cyclophosphamide. We next evaluated DC101 activity in *neu*-N mice, which exhibit profound peripheral immune tolerance to neu and thus represent a more clinically relevant model. DC101 treatment of tumor-bearing *neu*-N mice inhibited angiogenesis, induced apoptosis, and increased serum VEGF

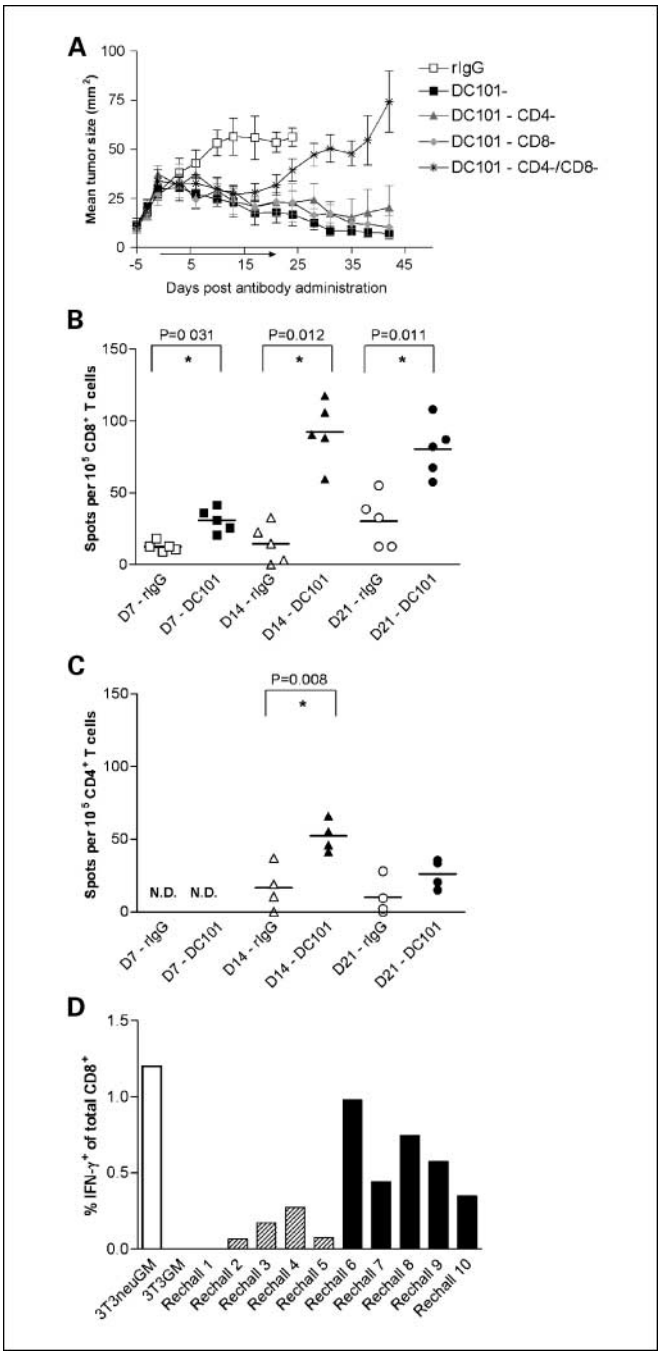

Fig. 4. DC101 treatment inhibits tumor growth by a T cell – dependent mechanism in FVB mice. *A,* the experiment in Fig. 1B, where tumor-bearing FVB mice received antibodies for 3 wks, was repeated in the setting of T cell depletion. Additional groups ($n = 10$) were included, where before receiving DC101, $CD4^+$ and $CD8^+$ T cells were depleted either individually ($CD4^-$ and $CD8^-$) or together ($CD4^-/CD8^-$). The data shown represent the averaged values for DC101-treated mice in the presence and absence of combined CD4 and CD8 depletion (two replicates). The individual CD4 and CD8 depletions were done once with the second evaluation of combined depletion. In one experiment, the group of mice treated with DC101 was followed to cure, with 100% tumor rejection (data not shown). *B* and *C,* splenic T cells were isolated from tumor-bearing FVB mice at 1, 2, and 3 wks after antibody administration ($n = 5$ per group). The $CD8^+$ and $CD4^+$ effector T cells (*B* and *C,* respectively) were then incubated with NT2.5B7.1 target cells for an IFN-γ ELISPOT. Symbols, individual mice; line, average. N.D. = not detected. *D,* DC101-treated FVB mice that completely rejected tumor (data not shown) were rechallenged and followed for 1 mo. At that time, half of the mice had developed tumors (*striped columns*), and half remained tumor free (*solid columns*). Splenic T cells were then isolated, and reactivity to $RNEU_{420-429}$ was determined by IFN-γ ICS. Controls included FVB mice given a neu-specific vaccine (*3T3neuGM*) or a mock vaccine (*3T3GM*).

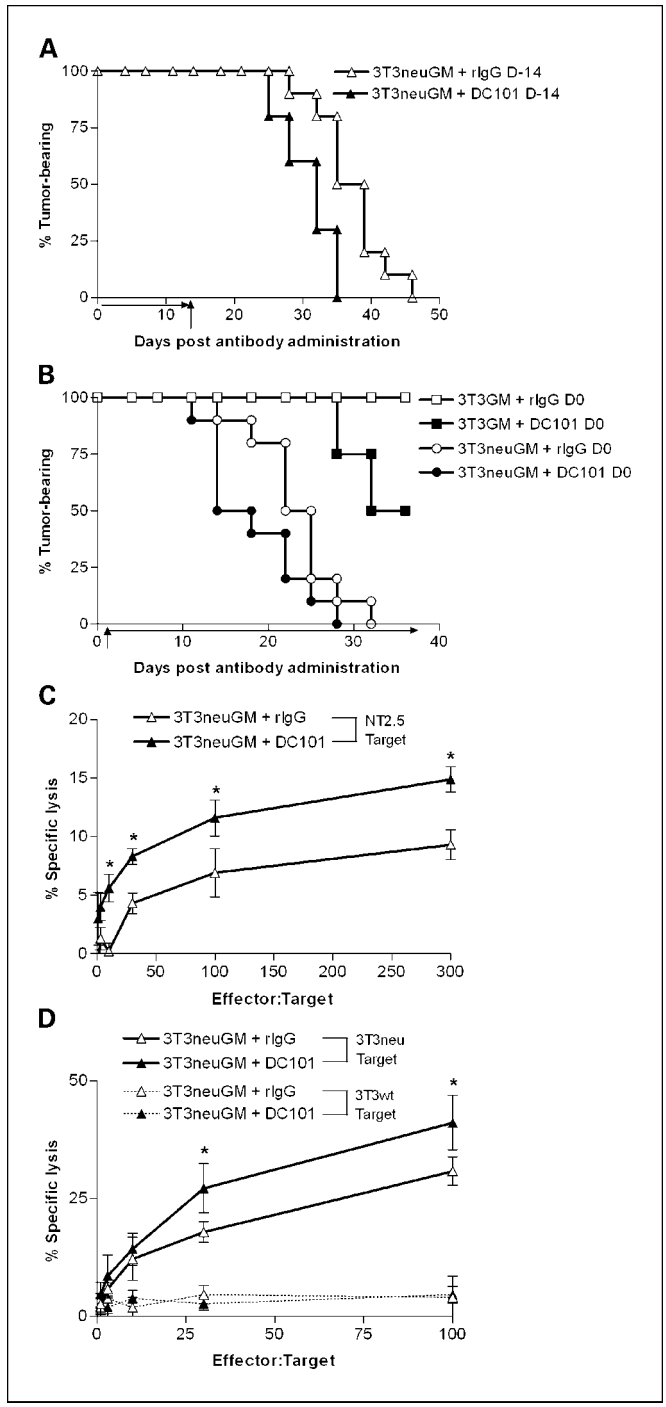

Fig. 5. Combining DC101 and neu-specific vaccination improves antitumor responses and CTL activity in FVB mice. *A,* FVB mice ($n = 10$ per group) were tumor challenged and 2 wks later received a 2-wk course of DC101 or rIgG (*horizontal arrow*), followed by vaccination (*3T3neuGM*; *vertical arrow*). *B,* FVB mice ($n = 10$ per group) were tumor challenged and 2 wks later were vaccinated and began receiving either DC101 or rIgG on the same day. *C* and *D,* 2 wks postvaccination, splenic effector T cells were isolated from mice in *A* ($n = 5$) and used in a 4-h chromium-release assay with NT2.5B7.1 cells (*C*) or 3T3neuB7.1 cells (*D*) as targets to detect tumor-specific and neu-specific lysis, respectively. 3T3 cells, lacking the neu antigen, were used as a negative control. *, $P < 0.05$.

levels without affecting MSCs or DCs (data not shown). Moreover, the rate of tumor growth was significantly reduced in tumor-bearing DC101-treated *neu*-N mice compared with rIgG-treated controls (Fig. 6A).

In contrast to DC101-induced tumor regression in FVB mice, tumors in *neu*-N mice continued to grow slowly during DC101 treatment (day 0: 23.7 ± 4.7 mm^2; day 21: 33.7 ± 6.4 mm^2; $P < 0.05$) and then upon discontinuing DC101 (Fig. 6A). Also, unlike FVB mice, tumor-specific $CD8^+$ T cells did not significantly expand in DC101-treated *neu*-N mice (data not shown), and there was no difference in tumor growth in DC101-treated neu-vaccinated and mock-vaccinated *neu*-N mice (Fig. 6B).

One strategy used to overcome tolerance in *neu*-N mice is immune modulation with low-dose cyclophosphamide and doxorubicin (25). Cyclophosphamide selectively depletes cycling $CD4^+CD25^+$ Tregs, leading to improved tumor-free survival and vaccine-induced neu-specific T cell activation in vaccinated *neu*-N mice (12). With each chemotherapeutic agent given as a single dose 1 week apart, it is unlikely that endothelial cells are selectively targeted by this timed sequential chemotherapy (as described in some metronomic chemotherapy regimens; ref. 31).

Depleting Tregs before vaccination could uncover the ability of DC101 to improve the efficacy of neu-specific vaccination in *neu*-N mice. We found that combining DC101 and chemotherapy-modulated neu-specific vaccination resulted in the highest tumor-free survival rate to date in vaccinated *neu*-N mice at 40% compared with 10% with chemotherapy-modulated neu-specific vaccination alone ($P = 0.022$) or 0% with DC101 and chemotherapy-modulated mock vaccination ($P < 0.05$; Fig. 6C). Although immune responses to the neu antigen were not significantly improved after incorporating DC101 into the chemotherapy-vaccine regimen (data not shown), the enhanced *in vivo* antitumor response did correlate with a small but statistically significant increase in CTL activity specific for NT2.5 tumor cells (Fig. 6D). These observations suggest that DC101 combined with immune modulation and vaccination in *neu*-N mice could augment the activity of tumor-specific T cells overall. These data also provide evidence that, in the appropriate context (i.e., absence of immune tolerance), DC101 can be effectively integrated with vaccination, enhancing both tumor-free survival and antitumor immune responses.

Discussion

The data presented here support three new findings. First, DC101 alone can induce T cell–mediated antitumor immune responses leading to tumor rejection in the absence of immune tolerance; both $CD4^+$ and $CD8^+$ T cells contribute to this effect. Second, combining DC101 and tumor-specific vaccination can induce greater immune responses than either therapy alone. Third, DC101 does not induce systemic VEGF-mediated immune suppression or inhibit the infiltration of TIL in this model. Importantly, this is the first study to systematically

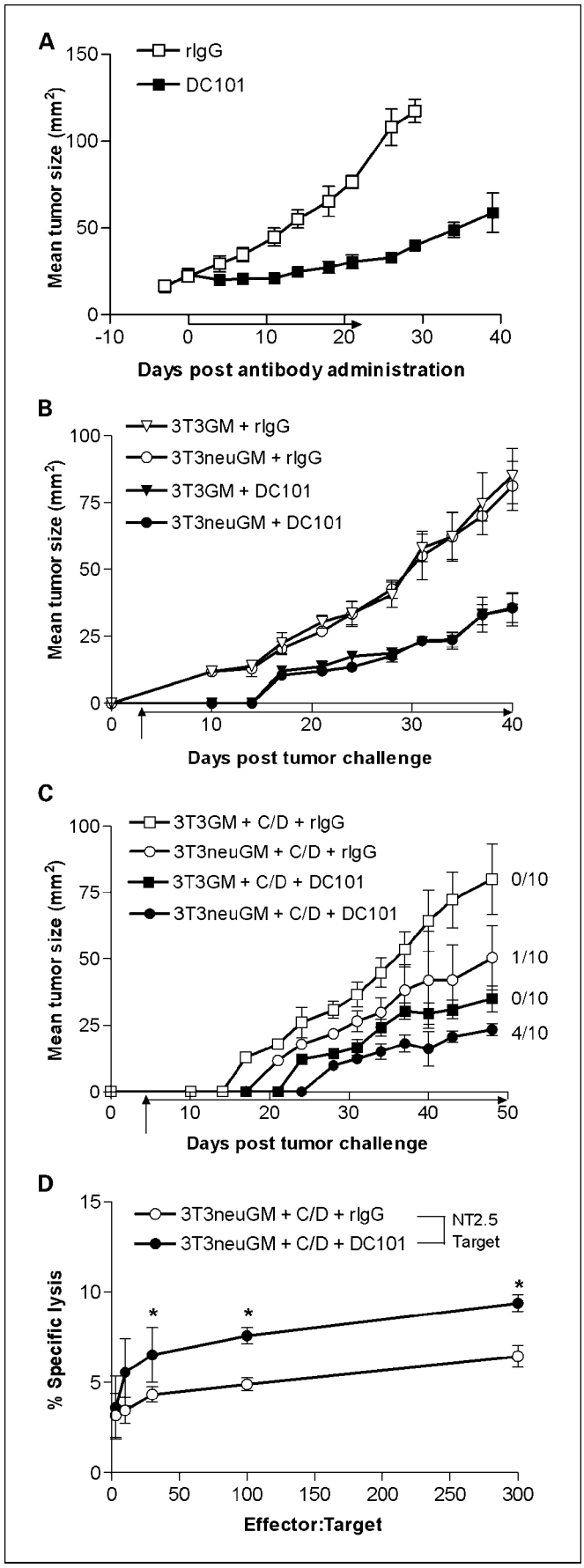

Fig. 6. DC101 enhances antitumor responses in *neu*-N mice only when immune tolerance is modulated by elimination of Tregs. *A,* tumor-bearing *neu*-N mice ($n = 20$ per group) received rIgG or DC101 biweekly for 3 wks (*horizontal arrow*). *B, Neu*-N mice ($n = 10$ per group) were tumor challenged, and 3 d later, mice were vaccinated and received rIgG or DC101 biweekly for the duration of the experiment. *C, Neu*-N mice ($n = 10$ per group) were tumor challenged, vaccinated, and given antibody as described in (*B*). However, immune modulation with low-dose cyclophosphamide and doxorubicin was also added (*C/D*). Listed next to each curve is the proportion of mice that remained tumor free at the end of the experiment (day 50). *D,* at the end of the experiment, splenic effector T cells were isolated and used in a 4-h chromium-release assay with NT2.5B7.1 cells as targets. *, $P < 0.05$.

examine tumor-specific immune responses after DC101 treatment and thus reveals the induction of an immune response as a novel antitumor activity mediated by DC101.

Most studies examining the therapeutic activity of DC101 have tested the antibody against human tumor xenografts in immune-deficient mice (32–35). These models show potent antiangiogenic effects, but are inherently unsuitable for detecting the immune activating potential of DC101. For example, whereas DC101 reduces the growth rate of tumors in nude mice compared with controls, most tumors are still slowly growing during and upon withdrawing DC101 treatment (19, 33). Improved tumor-free survival was recently described when DC101 was combined with DC-based vaccination in immune-competent mice; however, immune responses were not examined (36).

In our experiments, immune-competent mice are receiving the rat monoclonal antibody DC101. Tumors in FVB mice regress both during and after DC101 treatment, suggesting that any neutralizing antibodies specific for DC101 present do not impact its antitumor effect.

Our model system offers the opportunity to examine immune responses in both the absence (FVB mice) and presence (*neu*-N mice) of immune tolerance against the neu tumor antigen. Here, we show for the first time that DC101 can induce T cell–dependent tumor regression in immune-competent FVB mice (which do not exhibit antigen-specific immune tolerance). The strong immunogenicity of the neu antigen in FVB mice might lead to effective antigen presentation, thereby augmenting T cell activation and promoting tumor regression. In contrast, the ability of DC101 to augment neu-specific immune responses may be minimal in *neu*-N mice due to preexisting mechanisms of immune tolerance. In fact, DC101 merely slowed tumor growth, but induced neither frank tumor regression nor tumor-specific immune responses in *neu*-N mice. Moreover, Treg depletion with cyclophosphamide given before vaccination was required to allow DC101 to enhance vaccine-induced tumor regression responses in *neu*-N mice. This response correlated with very modest, but statistically significant, increases in tumor-specific CTL-mediated lysis. The impact of combined therapy on tumor-free survival in *neu*-N mice suggests that leveraging very small therapeutic gains in the setting of multitargeted therapy can result in a clinically meaningful therapeutic effect.

Notably, the ability of DC101 to mediate durable tumor regression in FVB mice seems to be T cell–dependent. DC101 treatment alone resulted in the significant expansion of tumor-specific $CD8^+$ T cells in immune-competent, nontolerant FVB mice. When DC101 was given to neu-vaccinated tumor-bearing FVB mice, there was enhanced lytic activity against tumor cells and cells expressing full-length neu protein, but an equivalent response to the immunodominant epitope $RNEU_{420-429}$. This suggests that heterogeneous epitopes from neu, and possibly other tumor antigens, may be presented to enhance DC101-mediated antitumor responses. Currently, we are working to identify alternate epitopes of neu that may be recognized. Finally, although the tumor-specific antibody titer did not change with DC101 treatment, it may also be possible that DC101 modulates the repertoire of the tumor-specific humoral immune response.

These data show that, in addition to its direct antiangiogenic activity, DC101 requires functional T cells to induce tumor-specific immune activation. Consistent with these data, the antiangiogenic agents endostatin and angiostatin can also enhance the antitumor response in immune-competent mice as compared with immune-deficient mice (37, 38). These observations together illustrate that the host immune system can contribute to the antitumor activity of antiangiogenic therapy.

At least two possible mechanisms may explain DC101-mediated immune activation. First, DC101 may enhance the cross-presentation of multiple neu-derived T cell epitopes by inducing tumor cell apoptosis (39). In fact, presentation of tumor-specific antigens after apoptosis has been shown to result in cross-priming both *in vitro* and *in vivo* (40–43). Alternatively, $CD8^+$ T cells may be primed directly by DC101-treated tumors. DC101 could induce up-regulation of costimulatory molecules or cytokines within the tumor microenvironment to improve direct priming. This has been shown for other cancer therapies such as low-dose melphalan, mitomycin C, and gamma-irradiation (44, 45). Further studies are now under way to explore the mechanism of DC101-mediated immune activation in FVB and *neu*-N mice.

We did not find evidence for VEGF-related immune suppression with DC101 treatment (15, 28). Others have shown that the administration of anti-VEGF neutralizing antibodies enhanced the effectiveness of tumor-specific immunotherapy by improving DC activity in murine models (46). High VEGF levels did not inhibit DCs in our model, consistent with data showing that DCs can exhibit different degrees of sensitivity to VEGF-mediated inhibition depending on the context of their stimulation (47). Moreover, in our model, the size of the immature myeloid cell population correlated with tumor burden rather than VEGF concentration. Because multiple cytokines regulate myeloid cell differentiation and expansion (27), activation of immune responses in DC101-treated mice might induce differentiation, whereas tumor-derived factors could promote expansion in rIgG-treated mice. It is also possible that the serum VEGF lacks bioactivity or the ability to bind VEGF-R1, which has been shown to mediate DC suppression (30).

Additionally, we hypothesized that T cells could still infiltrate DC101-treated tumors despite the inhibition of neovascularization because tumor regression was improved in DC101-treated mice. Evaluating the TIL revealed that DC101 does not inhibit, and may actually improve, T cell infiltration into the tumors of treated FVB mice. These data are consistent with recent work showing that DC101 can promote vascular normalization, where immature vessels are pruned and the remaining ones are strengthened (48). Normalization of aberrant tumor-associated vessels has been shown to increase the delivery of chemotherapeutic agents (49) and improve the trafficking of adoptively transferred T cells (50).

In conclusion, we show for the first time that DC101, in addition to its established antiangiogenic activity, can also elicit effective tumor-specific, T cell–mediated immune responses in the absence of immune tolerance. We also provide evidence that DC101 can be strategically combined with tumor immunotherapy to improve both tumor-free survival and tumor-specific immune responses. These data support the development of multitargeted treatments combining active vaccination and antiangiogenic therapy for clinical translation.

Acknowledgments

We thank Leslie Meszler for technical assistance with microscopy, and Drs. Drew Pardoll and Barry Kobrin for their critical review of this manuscript.

References

1. Walker LS, Abbas AK. The enemy within: keeping self-reactive T cells at bay in the periphery. Nat Rev Immunol 2002;2:11–9.
2. Nair S, Boczkowski D, Moeller B, Dewhirst M, Vieweg J, Gilboa E. Synergy between tumor immunotherapy and antiangiogenic therapy. Blood 2003;102:964–71.
3. Huang X, Wong MK, Yi H, et al. Combined therapy of local and metastatic 4T1 breast tumor in mice using SU6668, an inhibitor of angiogenic receptor tyrosine kinases, and the immunostimulator B7.2-IgG fusion protein. Cancer Res 2002;62:5727–35.
4. Huang X, Raskovalova T, Lokshin A, et al. Combined antiangiogenic and immune therapy of prostate cancer. Angiogenesis 2005;8:13–23.
5. Ellis LM, Liu W, Ahmad SA, et al. Overview of angiogenesis: biologic implications for antiangiogenic therapy. Semin Oncol 2001;28:94–104.
6. Ferrara N, Hillan KJ, Novotny W. Bevacizumab (Avastin), a humanized anti-VEGF monoclonal antibody for cancer therapy. Biochem Biophys Res Commun 2005;333:328–35.
7. Gupta K, Zhang J. Angiogenesis: a curse or cure? Postgrad Med J 2005;81:236–42.
8. Brand FX, Ravanel N, Gauchez AS, et al. Prospect for anti-HER2 receptor therapy in breast cancer. Anticancer Res 2006;26:463–70.
9. Guy CT, Webster MA, Schaller M, Parsons TJ, Cardiff RD, Muller WJ. Expression of the neu protooncogene in the mammary epithelium of transgenic mice induces metastatic disease. Proc Natl Acad Sci U S A 1992;89:10578–82.
10. Reilly RT, Gottlieb MB, Ercolini AM, et al. HER-2/neu is a tumor rejection target in tolerized HER-2/neu transgenic mice. Cancer Res 2000;60:3569–76.
11. Ercolini AM, Machiels JP, Chen YC, et al. Identification and characterization of the immunodominant rat HER-2/neu MHC class I epitope presented by spontaneous mammary tumors from HER-2/neu-transgenic mice. J Immunol 2003;170:4273–80.
12. Ercolini AM, Ladle BH, Manning EA, et al. Recruitment of latent pools of high avidity $CD8^+$ T cells to the anti-tumor immune response. J Exp Med 2005;201:1591–602.
13. Murata S, Ladle BH, Kim PS, et al. OX40 costimulation synergizes with GM-CSF whole-cell vaccination to overcome established $CD8^+$ T cell tolerance to an endogenous tumor antigen. J Immunol 2006;176:974–83.
14. Ferrara N, Gerber HP, LeCouter J. The biology of VEGF and its receptors. Nat Med 2003;9:669–76.
15. Ohm JE, Carbone DP. VEGF as a mediator of tumor-associated immunodeficiency. Immunol Res 2001;23:263–72.
16. Brown LF, Berse B, Jackman RW, et al. Expression of vascular permeability factor (vascular endothelial growth factor) and its receptors in breast cancer. Hum Pathol 1995;26:86–91.
17. Sepp-Lorenzino L, Thomas KA. Antiangiogenic agents targeting vascular endothelial growth factor and its receptors in clinical development. Expert Opin Investig Drugs 2002;11:1447–65.
18. Shaheen RM, Tseng WW, Vellagas R. Effects of an antibody to vascular endothelial growth factor receptor-2 on survival, tumor vascularity, and apoptosis in a murine model of colon carcinomatosis. Int J Oncol 2001;18:221–6.
19. Prewett M, Huber J, Li Y, et al. Antivascular endothelial growth factor receptor (fetal liver kinase 1) monoclonal antibody inhibits tumor angiogenesis and growth of several mouse and human tumors. Cancer Res 1999;59:5209–18.
20. Correia-Neves M, Waltzinger C, Mathis D, Benoist CM. The shaping of the T cell repertoire. Immunity 2001;14:21–32.
21. Kouskoff V, Signorelli K, Benoist C, Mathis D. Cassette vectors directing expression of T cell receptor genes in transgenic mice. J Immunol Methods 1995;180:273–80.
22. Shimizu C, Kawamoto H, Yamashita M, et al. Progression of T cell lineage restriction in the earliest subpopulation of murine adult thymus visualized by the expression of lck proximal promoter activity. Int Immunol 2001;13:105–17.
23. Dranoff G, Jaffee E, Lazenby A, et al. Vaccination with irradiated tumor cells engineered to secrete murine GM-CSF stimulates potent, specific, long lasting antitumor immunity. Proc Natl Acad Sci U S A 1993;90:3539–43.
24. Altman JD, Moss PA, Goulder PJ, et al. Phenotypic analysis of antigen-specific lymphocytes. Science 1996;274:94–6.
25. Machiels JP, Reilly RT, Emens LA, et al. Cyclophosphamide, doxorubicin, and paclitaxel enhance the antitumor immune response of granulocyte/macrophage-colony stimulating factor-secreting whole-cell vaccines in HER-2/neu tolerized mice. Cancer Res 2001;61:3689–97.
26. Bocci G, Man S, Green SK, et al. Increased vascular endothelial growth factor (VEGF) as a surrogate marker for optimal therapeutic dosing of VEGF receptor-2 monoclonal antibodies. Cancer Res 2004;64:6616–25.
27. Bronte V, Serafini P, Apolloni E, Zanovello P. Tumor-induced dysfunctions caused by myeloid suppressor cells. J Immunol 2001;24:431–46.
28. Gabrilovich D, Ishida T, Oyama T, et al. Vascular endothelial growth factor inhibits the development of dendritic cells and dramatically affects the differentiation of multiple hematopoietic lineages *in vivo*. Blood 1998;92:4150–66.
29. Oyama T, Ran S, Ishida T, et al. Vascular endothelial growth factor affects dendritic cell maturation through the inhibition of nuclear factor-κB activation in hematopoietic progenitor cells. J Immunol 1998;160:1224–32.
30. Dikov MM, Ohm JE, Ray N, et al. Differential roles of vascular endothelial growth factor receptors 1 and 2 in dendritic cell differentiation. J Immunol 2005;174:215–22.
31. Kerbel R, Kamen B. The anti-angiogenic basis of metronomic chemotherapy. Nat Rev Cancer 2004;4:423–36.
32. Shaheen RM, Ahmad SA, Liu W, et al. Inhibited growth of colon cancer carcinomatosis by antibodies to vascular endothelial and epidermal growth factor receptors. Br J Cancer 2001;85:584–9.
33. Zhang L, Yu D, Hicklin DJ, Hannay JA, Ellis LM, Pollock RE. Combined anti-fetal liver kinase 1 monoclonal antibody and continuous low-dose doxorubicin inhibits angiogenesis and growth of human soft tissue sarcoma xenografts by induction of endothelial cell apoptosis. Cancer Res 2002;62:2034–42.
34. Sweeney P, Karashima T, Kim SJ, et al. Anti-vascular endothelial growth factor receptor 2 antibody reduces tumorigenicity and metastasis in orthotopic prostate cancer xenografts via induction of endothelial cell apoptosis and reduction of endothelial cell matrix metalloproteinase type 9 production. Clin Cancer Res 2002;8:2714–24.
35. Jung YD, Mansfield PF, Akagi M, et al. Effects of combination anti-vascular endothelial growth factor receptor and anti-epidermal growth factor receptor therapies on the growth of gastric cancer in a nude mouse model. Eur J Cancer 2002;38:1133–40.
36. Pedersen AE, Buus S, Claesson MH. Treatment of transplanted CT26 tumour with dendritic cell vaccine in combination with blockade of vascular endothelial growth factor receptor 2 and CTLA-4. Cancer Lett 2006;235:229–38.
37. Li M, Huang X, Zhu Z, et al. Immune response against 3LL Lewis lung carcinoma potentiates the therapeutic efficacy of endostatin. J Immunother 2001;24:472–81.
38. Li M, Huang X, Zhu Z, Zhao Q, Wong M, Gorelik E. The therapeutic efficacy of angiostatin against weakly- and highly-immunogenic 3LL tumors. In Vivo 2002;16:577–82.
39. Ackerman AL, Cresswell P. Cellular mechanisms governing cross-presentation of exogenous antigens. Nat Immunol 2004;5:678–84.
40. Hoffmann TK, Meidenbauer N, Dworacki G, Kanaya H, Whiteside TL. Generation of tumor-specific lymphocytes by cross-priming with human dendritic cells ingesting apoptotic tumor cells. Cancer Res 2000;60:3542–9.
41. Albert ML, Sauter B, Bhardwaj N. Dendritic cells acquire antigen from apoptotic cells and induce class I-restricted CTLs. Nature 1998;392:86–9.
42. Nowak AK, Lake RA, Marzo AL, et al. Induction of tumor cell apoptosis *in vivo* increases tumor antigen cross-presentation, cross-priming rather than cross-tolerizing host tumor-specific CD8 T cells. J Immunol 2003;170:4905–13.
43. Nowak AK, Robinson BW, Lake RA. Synergy between chemotherapy and immunotherapy in the treatment of established murine solid tumors. Cancer Res 2003;63:4490–6.
44. Sojka DK, Donepudi M, Bluestone JA, Mokyr MB. Melphalan and other anticancer modalities up-regulate B7-1 gene expression in tumor cells. J Immunol 2000;164:6230–6.
45. Foss FM. Immunologic mechanisms of antitumor activity. Semin Oncol 2002;29:5–11.
46. Gabrilovich DI, Ishida T, Nadaf S, Ohm JE, Carbone DP. Antibodies to vascular endothelial growth factor enhance the efficacy of cancer immunotherapy by improving endogenous dendritic cell function. Clin Cancer Res 1999;5:2963–70.
47. Takahashi A, Kono K, Ichihara F, Sugai H, Fujii H, Matsumoto Y. Vascular endothelial growth factor inhibits maturation of dendritic cells induced by lipopolysaccharide, but not by proinflammatory cytokines. Cancer Immunol Immunother 2004;53:543–50.
48. Tong RT, Boucher Y, Kozin SV, Winkler F, Hicklin DJ, Jain RK. Vascular normalization by vascular endothelial growth factor receptor 2 blockade induces a pressure gradient across the vasculature and improves drug penetration in tumors. Cancer Res 2004;64:3731–6.
49. Jain RK. Normalization of tumor vasculature: an emerging concept in antiangiogenic therapy. Science 2005;307:58–62.
50. Ganss R, Ryschich E, Klar E, Arnold B, Hammerling GJ. Combination of T-cell therapy and trigger of inflammation induces remodeling of the vasculature and tumor eradication. Cancer Res 2002;62:1462–70.